ADVANCED FUNCTIONAL MATERIALS

Supporting Information

for *Adv. Funct. Mater.,* DOI: 10.1002/adfm.202100576

Biocompatible Light Guide-Assisted Wearable Devices for Enhanced UV Light Delivery in Deep Skin

Hao Zhang, Hangbo Zhao, Xingyue Zhao, Chenkai Xu, Daniel Franklin, Abraham Vázquez-Guardado, Wubin Bai, Jeffrey Zhao, Kan Li, Giuditta Monti, Wei Lu, Aya Kobeissi, Limei Tian, Xin Ning, Xinge Yu, Sunita Mehta, Debashis Chanda, Yonggang Huang, Shuai Xu, Bethany E. Perez White,* and John A. Rogers**

Supporting Information

Biocompatible Light Guide-Assisted Wearable Devices for Enhanced UV Light Delivery in Deep Skin

Hao Zhang, Hangbo Zhao, Xingyue Zhao, Chenkai Xu, Daniel Franklin, Abraham Vázquez-Guardado, Wubin Bai, Jeffrey Zhao, Kan Li, Giuditta Monti, Wei Lu, Aya Kobeissi, Limei Tian, Xin Ning, Xinge Yu, Sunita Mehta, Debashis Chanda, Yonggang Huang, Shuai Xu, Bethany E. Perez White,* John A. Rogers**

Figure S1. Light emission spectrum of UVA LEDs.

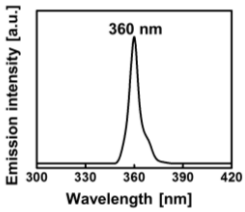

Figure S2. UV-visible transmittance of 1 mm-thick PLGA thin film.

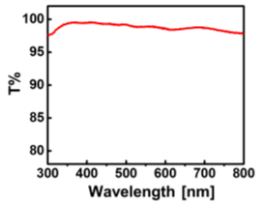

Figure S3. Scheme of fabrication steps of the microneedle light guides. The laser scribing step was performed by an external vendor.

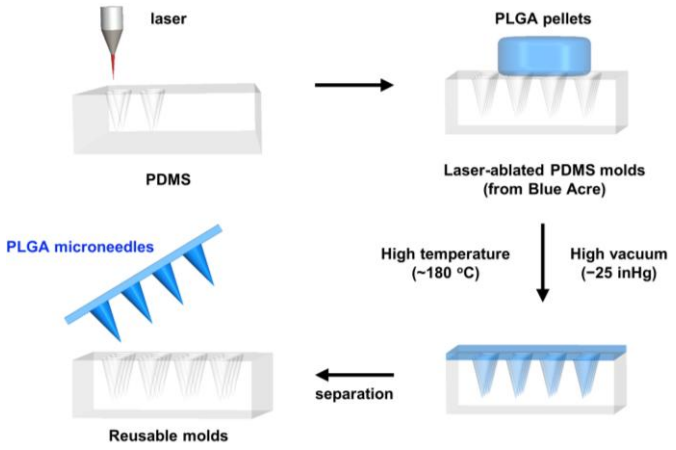

Figure S4. SEM **(a–d)** and optical images **(e–g)** of microneedle arrays with different configurations. (a–d) 1 mm-long microneedles with pyramidal shape and base/pitch sizes (in μm) of 200/300, 400/600, 300/400, and 400/500. Inset in (d) shows enlarged area highlighting a single microneedle. (e,f) Corresponding optical images of b and d. (g) Optical image of an array of conical microneedles with length of 2 mm, base diameter of 400 μm, and pitch size of 600 μm. Insets in (f,g) show magnified images. Scale bars in a–d: 500 μm; e–g: 1 mm.

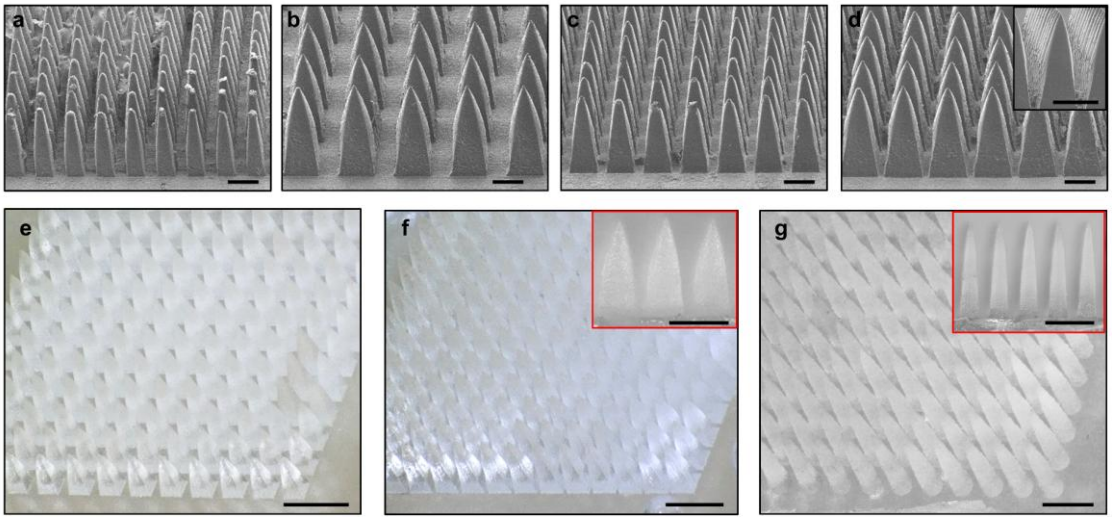

Figure S5. Measured light intensity of a battery-powered, skin-integrated system for UV-mediated skin therapy. A 45 mAh Li-ion battery supports the operation at ~100 mW cm^{-2} light intensity for more than 1 hour.

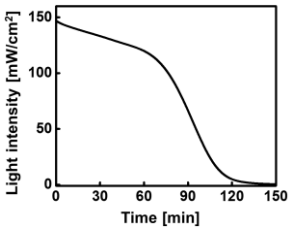

Figure S6. Pseudo-colored fluorescent image used in the spatial light distribution and mean light intensity analysis in Figure 2c,d. The color bar on the right shows the arbitrary light intensity.

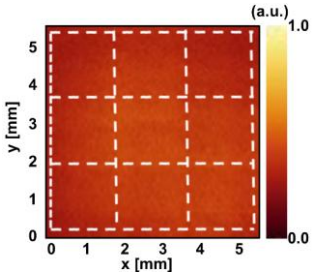

Figure S7. (a) Photograph of a bendable UVA LED patch on 12 μm-thick polyimide substrate laminated on a curved surface. Scale bar: 2 mm. **(b)** Current-voltage curves of bendable UVA LED patch in flat and bent states.

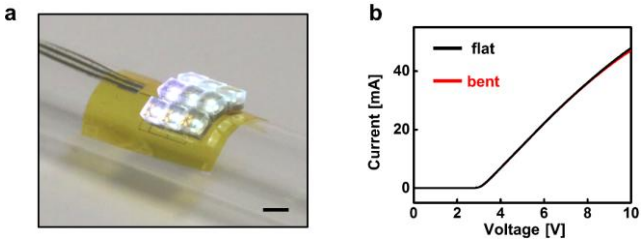

Figure S8. Photographs of two microneedle patches after repetitive insertion in porcine cadaver skin for different times. Most of the needles remain intact after these processes, though some of them undergo slight damage and deformation in the tip regions. Scale bars: 1 mm.

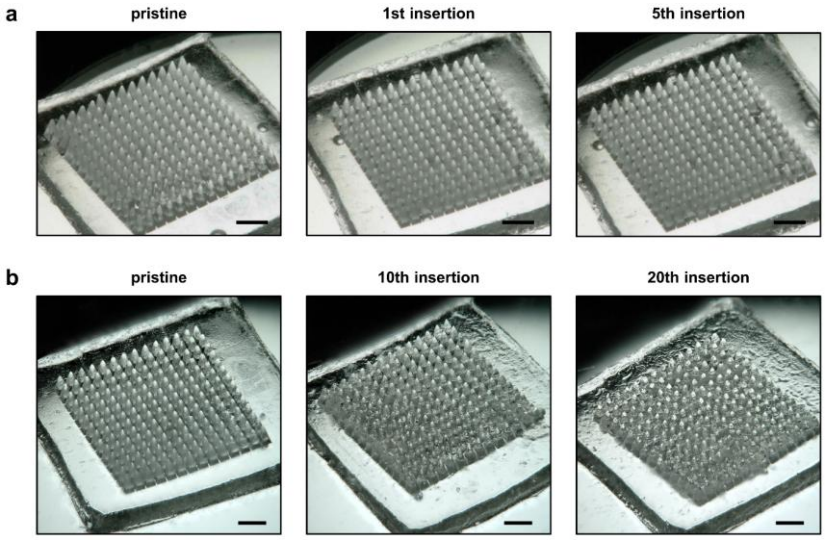

Figure S9. Distribution of **(a)** the strain and **(b)** stress of a single microneedle during skin insertion, as determined by the FEA analysis.

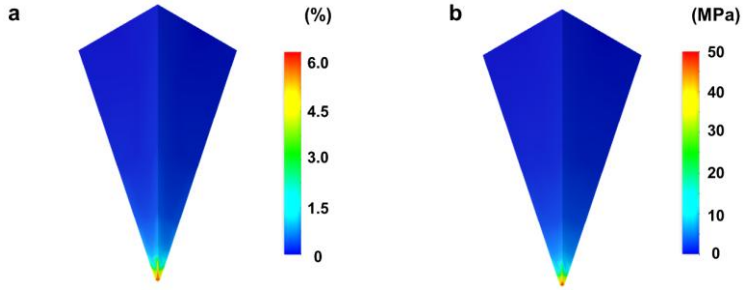

Figure S10. Stress-strain curves of handling layers of **(a)** unmodified PLGA and **(b)** PLGA after the solvent-based softening process.

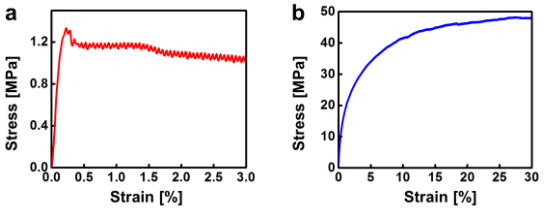

Figure S11. Photograph and FEA modeling of microneedles with the handling layer bent outward. Scale bar: 1 mm.

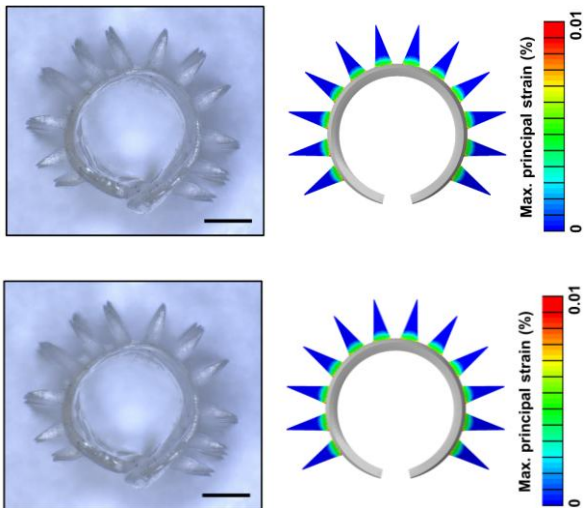

Figure S12. (a) Optical setup for measurement of light transport in porcine skin cadaver with or without microneedle light guides. **(b)** Pseudo-colored optical images taken when focused on the top surface of porcine skin cadaver (~1 mm thick) with or without microneedles. The blue dots correspond to the locations of the tips of microneedles. Scale bar: 1 mm. **(c)** Light intensity along lines (line 1 to 4, shown in the image on the top left). Peaks in the light intensity distribution correspond to the tips of microneedles. **(d)** Comparison of light intensities captured on the top surface of the porcine skin with or without microneedles.

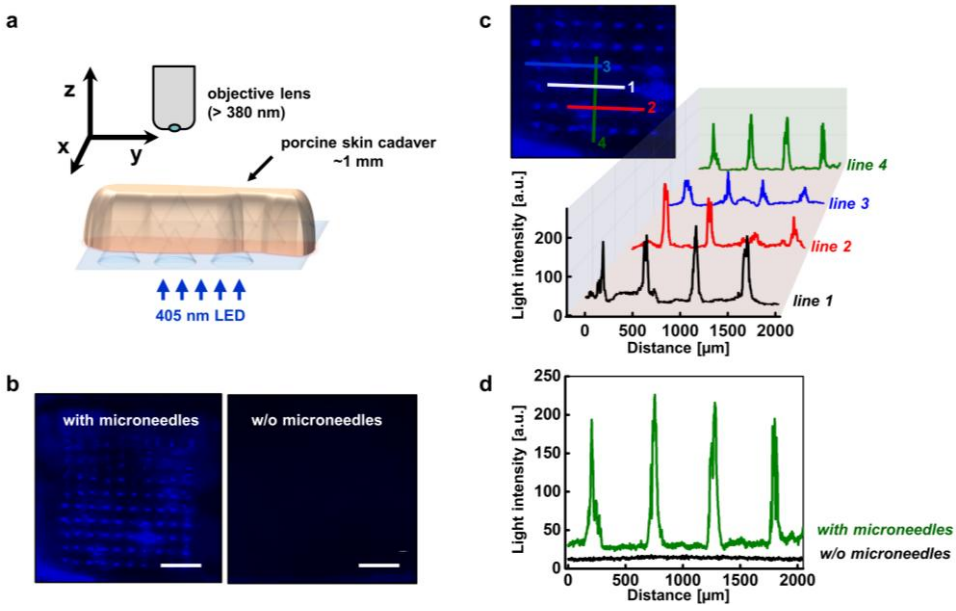

Figure S13. Simulated **(a)** total power and **(b)** the portion of power outside the microneedles (i.e., that effectively exposed to skin tissues) at various depths with different microneedle configuration under normal incident light. The length and tip size of all microneedle arrays are set to 1 mm and 10 μm. The base/pitch sizes are 200/300, 300/400, 400/500, and 400/600 μm, respectively. **(c)** Mean color intensity profiles of Figure 4e at various depths without or with microneedles (length/tip/base/pitch sizes of 1 mm/10 μm/400 μm/600 μm).

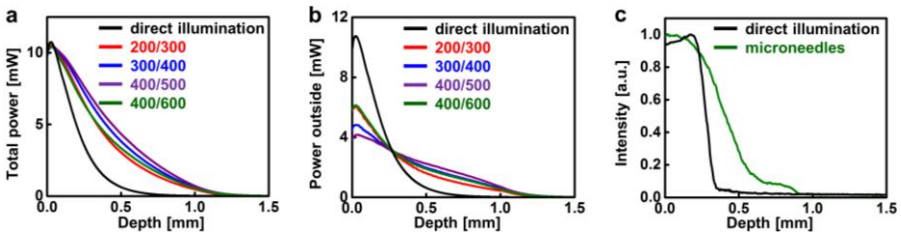

Figure S14. Comparison of Monte Carlo simulations of normalized 360 nm light intensity (Norm. Φ) distribution profiles in a turbid medium with optical properties close to human skin with different incident angles (0° and ±45°). The parameters of the **(a)** single microneedle or **(b)** array are length/tip/base/pitch sizes are 1 mm/10 μm/400 μm/600 μm. Color bar shows the logarithm scale of normalized light intensity in (a,b).

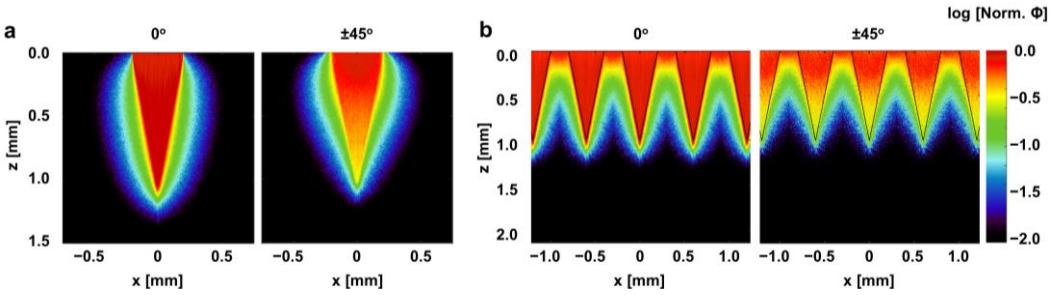

Figure S15. Monte Carlo simulation of normalized light intensity (Norm. Φ) distribution profiles in a turbid medium with optical properties close to human skin in the presence of microneedle guides with different configurations. The length and tip size of all microneedles are set to 1 mm and 10 μm. The base/pitch sizes are 200/300, 300/400, 400/500, and 400/600 μm, respectively, from left to right. The light source is 360 nm UV light with incident angle of 0^{o}. Color bar shows the logarithm scale of normalized light intensity.

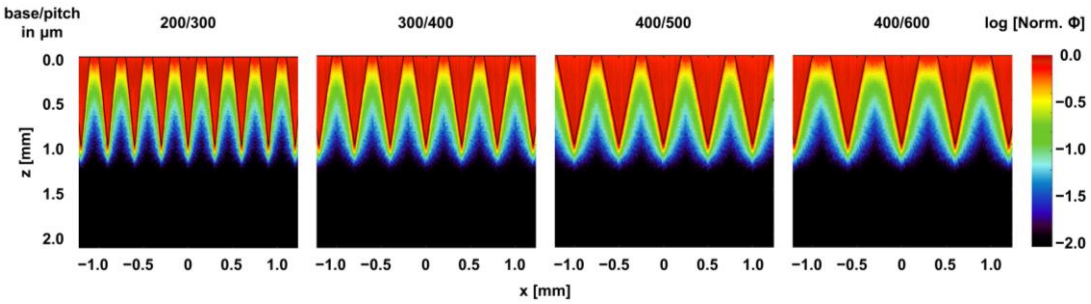

Figure S16. (a) Comparison of simulated light intensity delivered to skin (i.e., optical power outside the microneedles divided by the area of skin) at various depths with different microneedle configurations under normal incident light. The area of skin at various depths is calculated by subtracting the area occupied by microneedles from the total area of the microneedle patch (set as 7 mm × 7 mm). The length and tip size of all microneedle arrays are set to 1 mm and 10 μm. The base/pitch sizes are 200/300, 300/400, 400/500, and 400/600 μm, respectively. **(b)** Comparison of light intensity at incident angle of 0 and ±45°. The microneedle arrays used in (b) have length/tip/base/pitch sizes of 1 mm/10 μm/400 μm/600 μm.

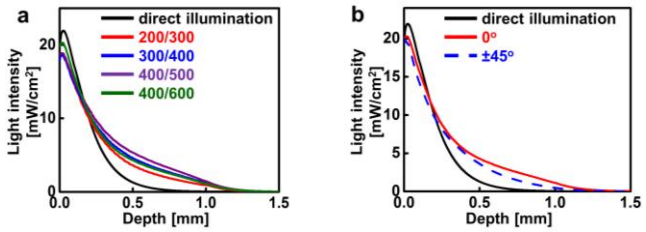

Figure S17. Measured optical properties (blue: absorbing coefficient, black: reduced scattering coefficient, and red: scattering anisotropy) of synthetic skin phantoms by using Inverse Adding-Doubling method. Skin phantoms with three different thickness (~1.0, 1.5, and 2.0 mm, from top to bottom) show similar optical parameters.

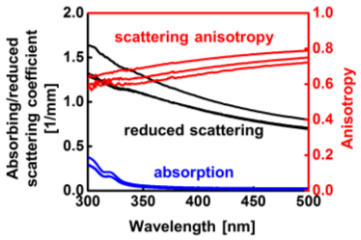

Table S1. Power of light (in mW) delivered at various depth intervals in the skin based on simulated results. Microneedle light guides have the configuration of base size = 400 μm, tip size = 10 μm, pitch size = 600 μm, and length = 1 mm. The highlighted rows correspond to dose in epidermis and the top dermis. These data were used to plot Figure 4d.

Depth intervals [μm]	Direct illumination [mW]	with microneedles [mW]
0–200	4.91	2.79
200–300	2.33	1.70
300–400	1.26	1.29
400–500	0.66	1.00
500–600	0.32	0.77
600–700	0.16	0.66
700–800	0.08	0.54
800–900	0.04	0.45
900–1000	0.02	0.37
1000–1100	0	0.26
1100–1200	0	0.15
1200–1300	0	0.07
1300–1400	0	0.04
1400–1500	0	0.02